PHYSICAL REVIEW B VOLUME 59, NUMBER 8 15 FEBRUARY 1999-II

Creation of highly anisotropic wave packets in quantum wells: Dynamical Franz-Keldysh effect in the optical and terahertz regimes

S. Hughes* and D. S. Citrin
Department of Physics and Materials Research Center, Washington State University, Pullman, Washington 99164-2814
(Received 31 August 1998)

We study the dynamical Franz-Keldysh effect by subjecting a semiconductor quantum well to both a strong THz-frequency driving field and a weak broadband optical pulse. Coulombic effects and the THz field are included nonperturbatively. Our results show THz sidebands in the optical absorption spectrum and harmonically generated subpicosecond bursts of radiation in the THz regime. The propagating wave packets are simultaneously analyzed and applications are discussed. [S0163-1829(99)50604-8]

The dynamical manifestations of interacting quasiparticles in an intense, low-frequency field may strongly affect the optical properties of a semiconductor in the vicinity of the absorption edge. One example that was predicted more than four decades ago is the Franz-Keldysh effect[1] (FKE). The FKE, i.e., the change in optical absorption due to the application of a static electric field in a periodic solid, is well established; namely, a strong dc electric field induces absorption below the band edge and oscillatory behavior of the absorption above. A direct dynamical analog of the FKE, the dynamical FKE (DFKE),[2] was recently introduced. It was predicted that the zero-field density of states (related to the absorption) splits off into replicas when a sample is placed in a strong THz field; the work was performed within the framework of nonequilibrium Green's functions and only continuum effects were included (i.e., no excitons). Qualitatively, similar structures were observed recently[3] by subjecting an optically excited semiconductor quantum well (QW) to an intense THz field from a free-electron laser (FEL); more strikingly, it was demonstrated that in the THz regime, a series of harmonically generated sidebands appears.

The purpose of this study is twofold: First, we introduce results based on the semiconductor-Bloch equations (SBE) in the presence of both an intense THz field and a broadband (50 fs) optical probe pulse excited at the band edge; this approach also allows us to analyze the creation and evolution of highly anisotropic electron-hole (e-h) *relative motion* wave packets (WP's), and, simultaneously, calculate the THz dynamics. The THz-field and excitonic effects are included nonperturbatively. Second, we develop a much simpler approach[4] that exhibits the same qualitative behavior; this contradicts theoretical works that claim the necessity of nonequilibrium Green's functions to explain the DFKE.[2]

Studies of the DFKE are timely since THz fields are readily available.[5] Indeed, THz fields can couple strongly with various elementary and collective intraband excitations to alter significantly the interband optical properties; for example, to achieve ultra-high-speed optical switching.[6] Moreover, two-color radiation methods (THz and near-IR) applied to mesoscopic semiconductors[7] have been recently developed. To characterize accurately and optimize the performance of the DFKE as well as to aid the development of related novel semiconductor devices, ultimately one has to understand the basic physical mechanisms. The investigation of interplaying THz and optical fields is also of general interest because it is connected to Coulomb many-body processes, such as excitonic effects, carrier transport phenomena, and electron correlations.

In the following, we assume a two-band QW where each e-h state with relative wave number $\mathbf{k}$ contributes to the total polarization $P=2A^{-1}\Sigma_{\mathbf{k}}d_{\mathrm{cv}}P_{\mathbf{k}}$, with d_{cv} the interband dipole matrix element. To obtain $P_{\mathbf{k}}$ we solve the SBE numerically, treating the influence of a *strong* THz field under optical excitation by a *weak* broad-band optical pulse. The SBE (Refs. 8 and 9) for the *slowly varying* polarization can be written in the low density limit ($\hbar=1$),

$$\left(\frac{\partial}{\partial t}+e\mathbf{F}_{\mathrm{THz}}(t)\cdot\boldsymbol{\nabla}_{\mathbf{k}}\right)P_{\mathbf{k}}=-i\Delta_{\mathbf{k}}P_{\mathbf{k}}+i\Omega_{\mathbf{k}}+\left.\frac{\partial P_{\mathbf{k}}}{\partial t}\right|_{\mathrm{cc}}, \quad (1)$$

with $\Delta_{\mathbf{k}}=E_{\mathbf{k}}-\omega_l$ the energy dispersion for a parabolic two-band semiconductor with unrenormalized transition energy $E_{\mathbf{k}}$, and $\omega_l=E_{\mathrm{gap}}$ the carrier frequency of the optical probe pulse assumed to be excited resonant with the band edge. The generalized Rabi frequency is $\Omega_{\mathbf{k}}=d_{\mathrm{cv}}\tilde{F}_{\mathrm{Opt}}(t)+\Sigma_{\mathbf{q}}V_{\mathbf{k}-\mathbf{q}}P_{\mathbf{q}}$, with $\tilde{F}_{\mathrm{Opt}}(t)$ the slowly varying optical field polarized in the QW plane, and $V_{\mathbf{q}}$ the Coulomb potential; $\mathbf{F}_{\mathrm{THz}}(t)$ is the THz field that is also assumed to be polarized in the QW plane. In general, Coulomb correlations (cc) between the carriers must be taken into account; in this paper we treat the dephasing of the optical polarization within the relaxation-time approximation,[10] $\dot{P}_{\mathbf{k}}|_{\mathrm{cc}}=-\gamma_o^{\mathrm{p}}P_{\mathbf{k}}$ where γ_o^{p} is the total dephasing rate of the optical polarization. For our theoretical approach the dynamics including the THz field can be treated exactly by introducing a moving coordinate frame $\tilde{t}=t,\tilde{\mathbf{k}}=\mathbf{k}+e\int^t\mathbf{F}_{\mathrm{THz}}(t')dt'$.[11] Terahertz-induced dephasing (TID) is acounted for via ionization of the exciton, as the electrons and holes get driven apart. For all following numerical calculations we choose parameters suitable for $\mathrm{In}_x\mathrm{Ga}_{1-x}\mathrm{As/GaAs}$ QW's: namely, reduced mass, $\mu=0.035\,m_e$; $1s$ [two-dimensional (2D)] excitonic binding energy, $E_{1s}\approx 11$ meV, $\gamma_o^{\mathrm{p}}\approx 500$ fs; and Bohr radius, $a_0=150$ Å. $\mathrm{In}_x\mathrm{Ga}_{1-x}\mathrm{As/GaAs}$ QW's are advantageous since with compressive strain one can increase the splitting of the heavy- and light-hole exciton.

In the linear regime, when a semiconductor is excited by a broadband optical pulse at the band edge, e-h pairs are

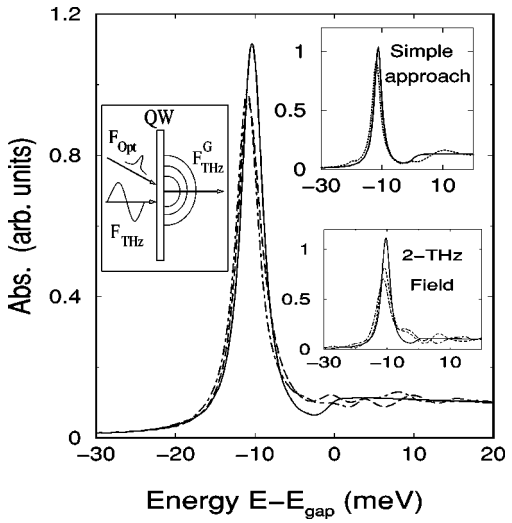

FIG. 1. The left inset shows the modeled experiment. The main figure shows the calculated optical absorption spectrum corresponding to no applied THz field (solid curve); with THz field and $\delta(t)=2\pi\nu_{\mathrm{THz}}t$ (chain curve); and with a THz field and $\delta(t)=2\pi\nu_{\mathrm{THz}}t+\pi/2$ (dot-dashed curve). The upper right inset shows the calculated absorption with and without the THz [$\delta(t)=2\pi\nu_{\mathrm{THz}}t$] field calculated using a simple equilibrium Green's function approach. The frequency and magnitude of the THz field is 1 THz and 3 kV/cm, respectively. The lower right inset shows identical calculations of the DFKE as in the main figure but with a 2 THz driving field of magnitude 6 kV/cm.

created with excess energy since the pulse bandwidth may extend tens of meV above E_{gap}. By simultaneously applying a THz field, the e-h pairs move in a highly complex manner depending on such effects as the electric field, the excitonic binding energy, and the geometry. Initially when the optical pulse arrives, an instantaneous polarization is created for the photoexcited e-h pairs, and subsequently, the carriers undergo acceleration by the electric field for times shorter than the mean scattering times. Similar scenarios using bias fields applied in the growth direction of QW's have been used to create THz emission via optical rectification[5] (instantaneous polarization) and charge oscillations (heavy- and light-hole quantum beating).

For the applied THz field we assume $\mathbf{F}_{\mathrm{THz}}(t)=\hat{\mathbf{n}}_x F_0\cos\delta(t)=\hat{\mathbf{n}}_x F_0\cos(2\pi\nu_{\mathrm{THz}}t+\phi)$, with ϕ the phase of the driving field at $t=0$ (center of the optical probe pulse), F_0 is the magnitude of the THz field (taken to be 3 kV cm), $\hat{\mathbf{n}}_x$ is a unit vector in the QW plane, and $\nu_{\mathrm{THz}}=1$ THz—unless stated otherwise. The linear optical field is taken to be a sech pulse and of 50 fs full width at half maximum irradiance. In the left inset of Fig. 1 we show a schematic of the double-field excitation scheme. In the main figure the absorption coefficient versus the detuning of the optical field is plotted with respect to the unrenormalized band edge. The dashed curve is for $\phi=0$; the chain curve is for $\phi=\pi/2$. Clearly, the DFKE occurs—in agreement with Refs. 2 and 3—where sidebands appear above the excitonic resonance. The small oscillations below the exciton are very weak for our chosen parameter range but become more pronounced for higher THz fields (see lower right inset discussed below). Further, the sidebands obviously depend on the relative phase of the THz field (at $t=0$) with respect to the arrival of the optical pulse. The phase ϕ can be controlled if both $\mathbf{F}_{\mathrm{THz}}(t)$ and $\mathbf{F}_{\mathrm{Opt}}(t)$ are derived from the same initial pulse using solid-state sources, though little phase control can be expected from FEL's. At $t=0$, both free e-h pairs and excitons are excited optimally from the crystal ground state, and the phase of $\mathbf{F}_{\mathrm{THz}}(0)$ determines the subsequent dynamics of the WP's internal motion. As discussed later, the dynamics of that part of the WP derived from states above E_{gap} can be understood qualitatively in terms of the classical motion of a free particle. For $\phi=0$, the THz field is a maximum at the center of the optical pulse and the carriers have minimum kinetic energy; at times before and after this instant, carriers propagate through the continuum and harmonics of the driving field may be generated when carriers undergo Coulombic rescattering as they travel back towards the zero of the relative coordinate (which determines the optical properties). This clearly shows up in the absorption spectrum via a series of peaks. The situation is different for $\phi=\pi/2$, where the kinetic energy is a maximum at $t=0$ and the carriers are accelerated until some later time (500 fs for the chosen ν_{THz}). Consequently, the harmonics that show up in the absorption spectrum differ in phase with respect to those generated for $\phi=\pi/2$. For comparison we have also plotted the linear absorption obtained when $\mathbf{F}_{\mathrm{THz}}(t)=0$ and in addition to a broadening of the $1s$ exciton resonance, in contrast to the usual blueshift of the exciton obtained from the quadratic Stark effect,[12] a redshift occurs. This is in agreement with Ref. 13 where it was predicted that a redshift dominates when the ratio of the mean kinetic energy divided by the THz field is less than unity. For comparison, as an upper right inset in Fig. 1, a calculation of the linear spectrum with (dotted curve) and without (solid curve) the 1-THz field is depicted, using a much simpler wave function approach (discussed later). The lower right inset shows SBE calculations but with a 2 THz driving field of magnitude 6 kV/cm. Clearly a significant broadening of the main exciton resonance occurs due to ionization of the exciton (TID). Additionally, the below oscillations become more pronounced.

Next we calculate the THz-induced (intraband) dipole moment, $\mathbf{P}_{\mathrm{THz}}(t)=e\int d^2rP^*(\mathbf{r},t)\mathbf{r}P(\mathbf{r},t)=-2e\Sigma_{\mathbf{k}}P^*_{\mathbf{k}}i\nabla_{\mathbf{k}}P_{\mathbf{k}}$, and subsequently for the THz electric field, assuming a point source (the actual spatial dependence will depend on the geometry) $\mathbf{F}^{\mathrm{G}}_{\mathrm{THz}}(t)=-(c^2r)^{-1}\ddot{\mathbf{P}}_{\mathrm{THz}}(t)$. Further, to depict the e-h WP dynamics, we calculate the polarization density (quantum-mechanical probability density of finding an electron and hole separated by $\mathbf{r}$ at time t) from $|P(\mathbf{r},t)|^2=|\int d^2rP_{\mathbf{k}}\exp(-i\mathbf{k}\cdot\mathbf{r})|^2$. As an inset to Fig. 2 we show the emitted THz field versus t for the phases (at $t=0$, center of the optical pulse) of $\phi=0$ (solid curve) and $\pi/2$ (dashed curve). Each transient is approximately 1 ps in duration reflecting the combined effect of WP spreading and dephasing. In the EM spectra (Fig. 2), a series of harmonics separated in frequency by approximately $2\nu_{\mathrm{THz}}$ appear in the THz regime. It is also noteworthy that the estimated peak dipole moments are 300 eÅ and 400 eÅ per e-h pair for $\phi=0$ and $\pi/2$, respectively. These dipole moments are estimated to be substantially larger than those emitted in standard schemes for THz generation in QW's (charge oscillations and optical rectification); this stems from the fact that the wave functions can be displaced by much larger dis-

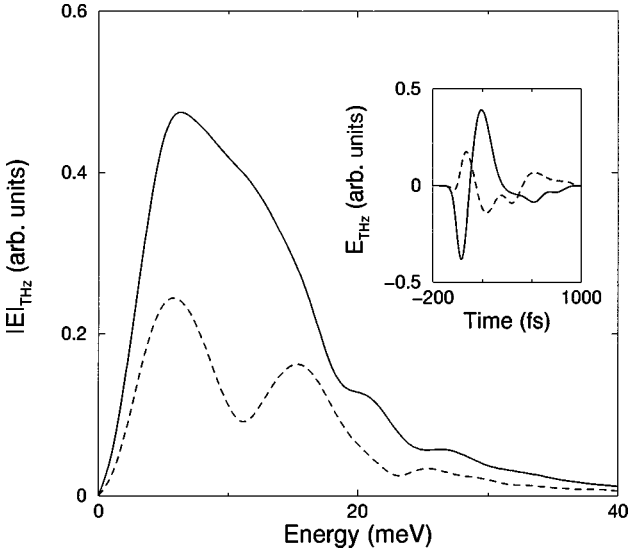

FIG. 2. Magnitude of the emitted THz spectra with $\delta(t)=2\pi\nu_{\mathrm{THz}}t$ (solid curve) and $\delta(t)=2\pi\nu_{\mathrm{THz}}t+\pi/2$ (dashed curve). The inset depicts the temporal behavior of the emitted THz field with $\delta(t)=2\pi\nu_{\mathrm{THz}}t$ (solid curve) and $2\pi\nu_{\mathrm{THz}}t+\pi/2$ (dashed curve). Note that an energy of 40 meV corresponds to a frequency of approximately 10 THz.

tances in the QW plane (see later) in comparison to a displacement in the growth direction, ~ 80 eÅ maximum (for 80 Å QW's) as limited by the QW width.

In Fig. 3 we show examples of the e-h WP (polarization density) at several snapshots in time corresponding to Fig. 1 ($\phi=0$); the driving field is linearly polarized in the x direction leading to the large asymmetry. Shortly after the optical pulse arrives ($t=100$ fs) the probability density is concentrated near the center (where there is a high probability of finding the electron and hole at the same relative position). Later ($t=250$ fs), beating between the excitonic and free-carrier WP is seen. Because the WP is highly anisotropic, there is a net dipole moment that results in the THz transients shown in Fig. 2. At later times ($t=400,640$ fs), sidelobes can be seen in the WP; these are formed by the combination of slow transverse spreading, the relatively fast field driven motion in the polarization direction, and the excitonic attraction (Coulombic rescattering). For reasonable driving fields of 3 kV cm, the e-h WP's can easily be displaced by 20 nm. In Fig. 4 we depict the WP dynamics for $\phi=\pi/2$. One recognizes that a significant amount of the WP has already propagated to the negative x direction (at $t=100$ fs). At $t=250$ fs the characteristic *moon* structure (due to beating) is obtained again, but the WP is much less pronounced at around 10 nm and has spread out more near the center than in Fig. 3. Later, one sees spatial interference in the relative-coordinate space.

Finally we explore a much simpler method for calculating the effects of the DFKE. One can construct the entire $\mathbf{r}$ and t dependence of the WP via $\psi(\mathbf{r},t)=\int_{-\infty}^{t}D(\mathbf{r},\mathbf{r}';t,t')\times dt'\mathbf{F}_{\mathrm{Opt}}(t')$, where $D(\mathbf{r},\mathbf{r}';t,t')$ is the Green's function of Eq. (1). In order to describe the *e-h* continuum, we assume that one can apply to $\psi(\mathbf{r},t)$ the classical equations of motion $\boldsymbol{\xi}(t)=-\xi_0\hat{\mathbf{n}}_x[\cos(\omega t+\phi)-\cos(\phi)+\omega t\sin(\phi)]$ for a free electron of reduced mass μ where $\xi_0=eF_0/\mu\omega^2$ is the amplitude of the induced displacement; both quiver and

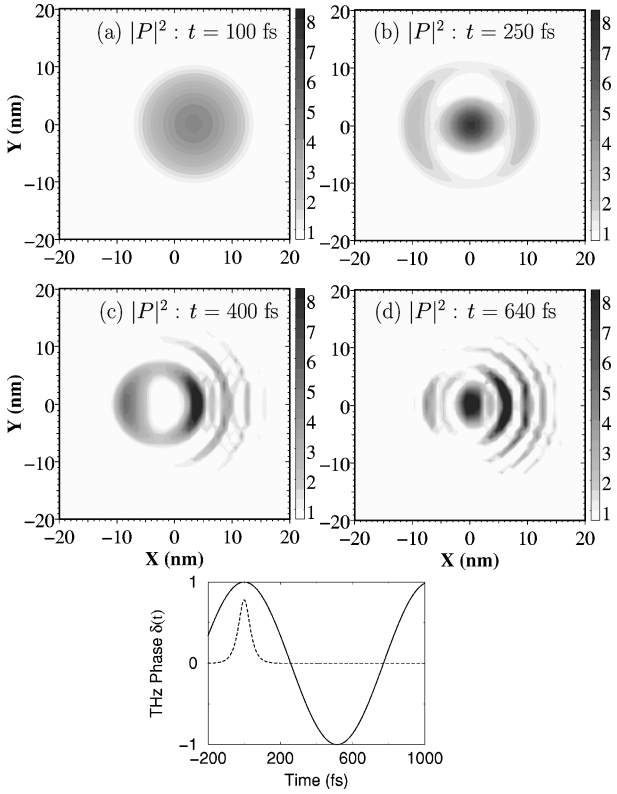

FIG. 3. (a) Wave packet at several times [(a) $t=100$ fs, (b) $t=250$ fs, (c) $t=400$ fs, and (d) $t=640$ fs] for the polarization density with $\delta(t)=2\pi\nu_{\mathrm{THz}}t$. The lower figure shows the THz-field phase (solid curve) and the optical pulse (dashed curve) versus time. The WP's are scaled by a factor of 10^3.

drift are included.[14] For the continuum contribution to the slowly-varying optical polarization we thus have $\tilde{\psi}_c(\mathbf{r},t)=\int_{\infty}^{t}D_c(\mathbf{r},\mathbf{r};t,t')dt'\tilde{F}_{\mathrm{Opt}}(t')\exp\{-i\omega_l(t'-t)\}$, where $D_c(\mathbf{r},\mathbf{r}';t,t')=-iK(\mathbf{r},\mathbf{r}';t,t')$ with $K(\mathbf{r},\mathbf{r}';t,t')$ the 2D free-particle propagator ($\hbar=1$):

$$K(\mathbf{r},\mathbf{r}';t,t')=\frac{\mu}{i2\pi(t-t')}\exp\left\{-i\left[(E_{\mathrm{gap}}-i\gamma_o^{\mathrm{p}})(t-t')-\frac{\mu}{2(t-t')}|\mathbf{r}-\boldsymbol{\xi}(t)-\mathbf{r}'+\boldsymbol{\xi}(t')|^2+\frac{\mu}{2}\int_{t'}^{t}dt''\dot{\xi}^2(t'')\right]\right\}\theta(t-t'). \quad (2)$$

Note that we have neglected the Sommerfeld factor in the continuum, which for realistic QW's has a rather weak effect. We take great care in handling the numerical singularity arising from the propagator. For the $1s$ exciton: $\tilde{\psi}_{1s}(\mathbf{r},t)=\int_{-\infty}^{t}D_{1s}(\mathbf{r},\mathbf{r}';t,t')dt'\tilde{F}_{\mathrm{Opt}}(t')\exp\{-i\omega_l(t'-t)\}$, where $D_{1s}(\mathbf{r},\mathbf{r}';t,t')=-i\varphi(\mathbf{r},t)\varphi^*(\mathbf{r}',t')\exp\{-i[(E_{1s}-i\gamma_o^{\mathrm{p}})(t-t')+\int_{t'}^{t}dt''\Delta_{1s}(t'')]\}\theta(t-t')$. The Stark shifted energy, $\Delta_{1s}(t)$,[4] and the modified $1s$ exciton wavefunction, $\varphi(\mathbf{r},t)$, are calculated self-consistently using standard perturbation theory; also, to account for TID, the dephasing rate was increased by 10%. Subsequently, the slowly-varying optical polarization can be obtained from $P(t)=[\tilde{\psi}_c(0,t)+\tilde{\psi}_{1s}(0,t)]d_{\mathrm{cv}}$. The wavefunction approach only yields a

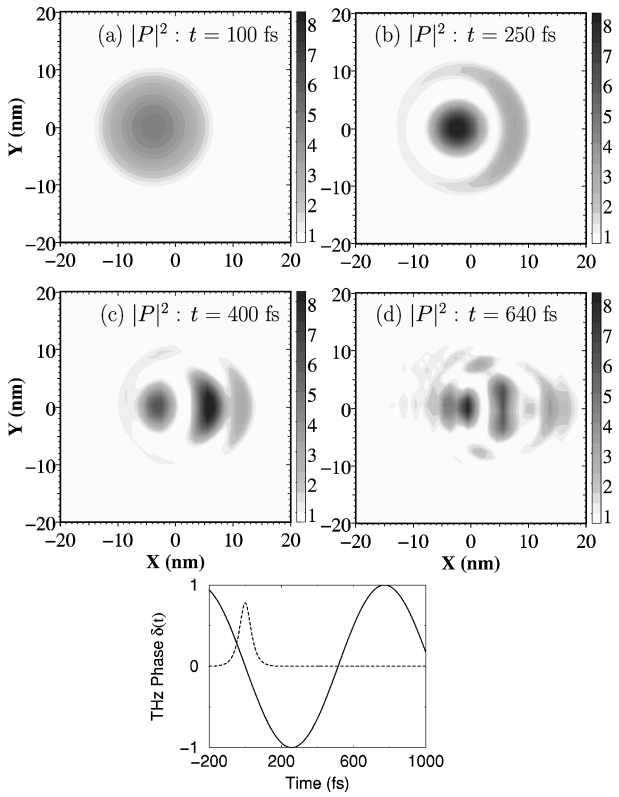

FIG. 4. As in Fig. 3 but with $\delta(t)=2\pi\nu_{\mathrm{THz}}t+\pi/2$.

semi-quantitative understanding of the full results but it is worth investigating due to its conceptual simplicity.

The upper right inset of Fig. 1 shows the computed absorption spectra with all material ($In_xGa_{1-x}As$) and field parameters as above. The solid curve corresponds to the usual scenario with $\mathbf{F}_{\mathrm{THz}}=0$, while the dotted curve represents the case with a THz field for $\delta(t)=2\pi\nu_{\mathrm{THz}}t$. Again, an excitonic redshift occurs and a series of harmonic structures appear in the optical absorption spectrum. The peaks between the exciton peak and the continuum are somewhat less pronounced than the SBE-calculations; this is probably due to a smaller probability for multi-photon absorption since we have neglected other excitonic transitions and Coulombic rescattering effects in the continuum. However, this simpler analysis is very appealing since unlike the numerical solution of the anisotropic SBE, it captures the essential physics while taking a negligible amount of CPU time. We have further verified that by changing the driving frequency to 2 THz then essentially all calculated peaks both above and below the fundamental exciton resonance obtained from the SBE are obtained with this approach.

In conclusion, we have theoretically investigated the simultaneous exposure of an $In_xGa_{1-x}As$ QW to a broadband optical pulse and a strong THz driving field. The scenario produces beating, e-h relative motion WP's whose anisotropic structure manifests in unique spectral and time-dependent features in both the optical and THz regimes. We verify the existence of the DFKE whose experimental signature appears via oscillations in the absorption above the band gap and a series of sideband frequencies resulting from nonlinear wavemixing. Besides being of interest on purely fundamental grounds, studies of THz generation and related phenomena have a host of applications including FIR/time-domain spectroscopy, study and control of Rydberg atoms, T-ray imaging of optical materials, laser-excited wave packets in heterostructures,[15] and the investigation of interplaying intraband and interband carrier dynamics.

We thank R. Zimmermann and T. B. Norris for enlightening discussions. This work was supporeted by the National Science Foundation by Grant No. DMR9705403 and the Office of Naval Research.

*Electronic address: shughes@wsu.edu

[1] W. Franz, Z. Naturforsch. A **13A**, 484 (1958); L. V. Keldysh, Zh. Eksp. Teor. Fiz. **34**, 1138 (1958) [Sov. Phys. JETP **34**, 788 (1958)].

[2] A. P. Jauho and K. Johnsen, Phys. Rev. Lett. **76**, 4576 (1996).

[3] K. B. Nordstrom *et al.*, Phys. Status Solidi B **204**, 52 (1997); and for the optical domain only, see K. B. Nordstrom *et al.*, Phys. Rev. Lett. **81**, 457 (1998).

[4] L. V. Keldysh, Zh. Eksp. Teor. Fiz. **47**, 1954 (1965) [Sov. Phys. JETP **20**, 1307 (1965)].

[5] S. L. Chuang *et al.*, Phys. Rev. Lett. **68**, 102 (1992); P. C. M. Planken *et al.*, *ibid.* **69**, 3800 (1992).

[6] S. Hughes and D. S. Citrin, Phys. Rev. B **58**, 15 969 (1998).

[7] J. Kono *et al.*, Phys. Rev. Lett. **79**, 1758 (1997).

[8] M. Lindberg and S. W. Koch, Phys. Rev. B **38**, 3342 (1988).

[9] I. Balslev *et al.*, Phys. Rev. B **40**, 4095 (1989).

[10] For a textbook discussion, see H. Haug and S. W. Koch, *Quantum Theory of the Optical and Electronic Properties of Semiconductors*, 3rd ed. (World Scientific, Singapore, 1994), and references therein.

[11] D. H. Dunlap and V. M. Kenkre, Phys. Rev. B **34**, 3625 (1986); T. Meier *et al.*, *ibid.* **51**, 14 490 (1995).

[12] D. Fröhlich *et al.*, Phys. Status Solidi B **173**, 83 (1992).

[13] K. Johnsen and A. P. Jauho, Phys. Status Solidi A **164**, 553 (1997).

[14] P. B. Corkum *et al.*, Phys. Rev. Lett. **62**, 1259 (1989).

[15] K. Leo and M. Koch, in The Physics and Chemistry of Wave Packets, edited by J. Yeazell (Wiley, New York, to be published).